Performance Enhancement of Smart Antennas with Reduced Element Spacing

H.J. Chaloupka and X. Wang
Dept. of Electrical Engineering and Information Technology
University of Wuppertal
Rainer-Gruenter Str. 21, D-42119 Wuppertal, Germany

J.C. Coetzee
Department of Electrical and Computer Engineering
National University of Singapore
4 Engineering Drive 3, Singapore 117576

***Abstract*— This paper addresses the problem of degradations in adaptive digital beam-forming (DBF) systems caused by mutual coupling between array elements. The focus is on compact arrays with reduced element spacing and, hence, strongly coupled elements. Deviations in the radiation patterns of coupled and (theoretically) uncoupled elements can be compensated for by weight-adjustments in DBF, but SNR degradation due to impedance mismatches cannot be compensated for via signal processing techniques. It is shown that this problem can be overcome via the implementation of a RF-decoupling-network. SNR enhancement is achieved at the cost of a reduced frequency bandwidth and an increased sensitivity to dissipative losses in the antenna and matching network structure.**

Keywords—adaptive beamforming; smart antennas; mutual coupling

I. INTRODUCTION

Antenna systems with digital beamforming (DBF) or so-called smart antennas provide a number of features which are not available with conventional phased-array antennas [1,2]:

(i) An antenna array with M operational antenna elements provides M mutually orthogonal radiation patterns (MORPs), each described by its angular dependence of amplitude, phase and polarization. By a weighted linear combination of these MORPs with complex-valued weights, an infinite set of radiation patterns in an M-dimensional space (space of available radiation patterns) can be formed.

(ii) Since the weighted linear combination is performed in the digital domain, an unlimited number of independent radiation patterns ("beams") can *simultaneously* be formed from the set of available patterns.

(iii) Features (i) and (ii) can be used to adaptively form radiation patterns which maximize the gain in a pre-specified direction of incidence (*beam forming*) and/or to spatially reject interference (*adaptive nulling*). Furthermore, the angular dependence of the pattern phase principally allows to coherently combine different multi-path-contributions from the same source. With multiport antennas at both the receiver and the transmitter side of a communication link (MIMO systems) multi-path contributions can be used to form parallel communication channels.

(iv) Imperfections in the analog part of the system can to some extent be corrected in the digital domain.

Fig. 1 depicts the architecture of a receiver system for DBF. It consists of a M-element antenna array, a set of M parallel receiver chains with analog-to-digital converters (ADCs) and the digital beamformer. Note, that only one beamformer is shown, but an arbitrary number of parallel beamformers can be implemented.

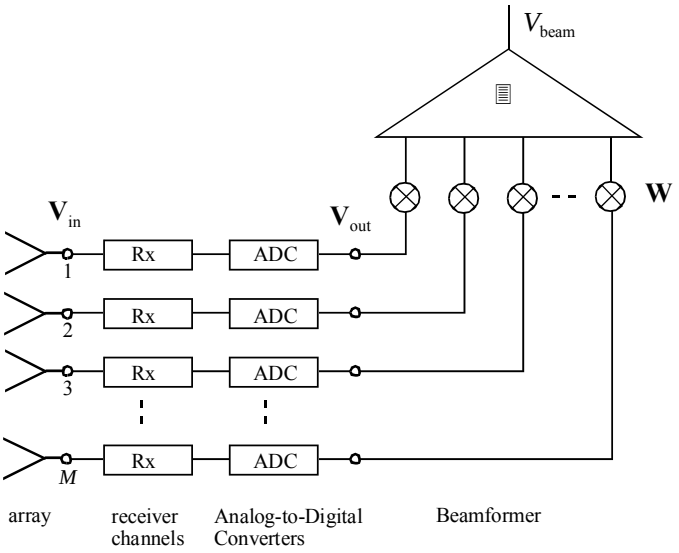

Fig. 1. Architecture of a receiver system for DBF comprising an antenna array with M antenna ports, M parallel receivers with ADCs and a digital beamformer. Some quantities which are used in the following theoretical considerations are depicted in this drawing,too.

It is well known that mutual coupling between the antenna elements leads to system performance degradation. This problem is even more severe if, due to size restrictions for the footprint diameter (platform-size) of the array, an element spacing significantly smaller than the conventional half-wave spacing is chosen. The most extreme case of this situation occurs if the available platform size is limited to a diameter on the order of 0.5λ. With conventional half-wave spacing, only one element (M=1) can be placed on this platform, preventing any kind of DBF. The number of degrees of freedom in DBF equals $M-1$. For maximum versatility, the number of elements needs to be as large as possible. However, the increased mutual coupling associated with the decreased element spacing gives rise to severe frequency bandwidth limitations and an increased sensitivity to dissipative losses. The required bandwidth and radiation efficiency thus limit the maximum number of elements for a given platform size.

The set of available radiation patterns of an array with reduced element spacing naturally differs from those of an array with conventional spacing. However, an array with M elements provides M mutually orthogonal patterns, independent of the element spacing.

This paper aims to provide a theoretical framework for modeling of performance degradation in DBF caused by an increased inter-element coupling in compact arrays of low order M. Furthermore, it presents a concept which makes it possible to partially overcome these effects and discusses the physical restrictions for the application of this concept.

II. MODELLING OF ARRAY PROPERTIES BY MEANS OF EIGENMODES AND EIGENPATTERNS

A. General case

An array with M operational elements can be described by the frequency-dependent $M\times M$ admittance matrix $\mathbf{Y} = \mathbf{G} + j\mathbf{B}$, which relates the M port currents I_n to the M driving port-voltages V_n. Mutual coupling occurs for non-vanishing off-diagonal elements, with the coupling between element m and element n characterized by matrix element Y_{mn} (with $m\neq n$). Modeling of array properties is significantly simplified if eigenmodes defined via the real-valued normalized and mutually orthogonal eigenvectors $\mathbf{x}_m$ of $\mathbf{G}$ are introduced:

$$\mathbf{G}\,\mathbf{x}_m = g_m \mathbf{x}_m \quad \text{with} \quad m = 1,\ldots M \tag{1}$$

If via

$$\mathbf{V} = \left(V_1, V_2, ..., V_M\right) = v_1\mathbf{x}_1 + v_2\mathbf{x}_2 + ... + v_M\mathbf{x}_M \tag{2}$$

the port-voltages V_n are expressed as a superposition of mode-voltages v_m , antenna input power becomes

$$P_{in} = \frac{1}{2}\sum_{m=1}^{M} g_m \left|v_m\right|^2 . \tag{3}$$

The corresponding free-space far field as a function of the distance r and the directions of observation Θ and Φ becomes

$$\mathbf{E} = \frac{\exp\left(-jk_0 r\right)}{2r}\sqrt{\frac{Z_0}{\pi}}\sum_{m=1}^{M}\sqrt{g_m}\,v_m\mathbf{C}_m\left(\Theta,\Phi\right) \tag{4}$$

with $\mathbf{C}_m$ the eigenpattern for mode m. In (4), $k_0 = 2\pi/\lambda$ and $Z_0 = 277\ \Omega$ denote the free-space wavenumber and the free space intrinsic impedance, respectively. Note that the vector functions $\mathbf{C}_m$ that define the eigenpatterns contain the angular dependency of amplitude, phase and polarization.

According to (4), $\left|\mathbf{C}_m\left(\Theta,\Phi\right)\right|^2$ represents the antenna gain-function associated with mode m. If dissipative losses in the antenna structure can be neglected, the radiated power becomes equal to the input power and this in turn leads to mutual orthogonal radiation pattern with

$$\oint \mathbf{C}_l\left(\Theta,\Phi\right)\cdot\mathbf{C}_m\left(\Theta,\Phi\right)d\Omega = 4\pi\delta_{lm} \tag{5}$$

By means of (1), M modes of the array with mutually coupled elements have been introduced. Each mode is associated with one of the M mutually orthogonal eigenpatterns and a corresponding mode conductance g_m.

B. Concept of mode-admittance for a special class of antennas

If the antenna structure possesses certain symmetry relations, the eigenvectors of $\mathbf{B}$ coincide with the eigenvectors of $\mathbf{G}$, so that

$$\mathbf{Y}\mathbf{x}_m = (\mathbf{G} + j\mathbf{B})\mathbf{x}_m = \left(g_m + jb_m\right)\mathbf{x}_m = y_m\mathbf{x}_m \tag{6}$$

A frequency-dependent mode-admittance $y_m = g_m + jb_m$ can thus be associated with mode m. A sufficient condition for an array to belong to this specific subclass of antennas is that all self-admittances Y_{nn} need to be equal to each other, and that the off-diagonal elements Y_{nm} only depend on $\left|n-m\right|$. A 3-element array with elements placed at the corners of a triangle with equal sides may serve as an example. With $Y_{11}=Y_{22}=Y_{33}$ and $Y_{12}=Y_{23}=Y_{13}$, the eigenvectors of this array become $\mathbf{x}_1^t = \left(1,1,1\right)/\sqrt{3}$, $\mathbf{x}_2^t = \left(2,-1,-1\right)/\sqrt{6}$ and $\mathbf{x}_3^t = \left(0,1,-1\right)/\sqrt{2}$. This leads to $y_1 = Y_{11} + 2Y_{12}$ and $y_2 = y_3 = Y_{11} - Y_{12}$ as the mode-admittances of modes 1 to 3.

By means of the eigenmode representation, the actual array with M mutually coupled elements can formally be replaced with a set of M uncoupled equivalent antennas. The mth equivalent antenna possesses the mth eigenpattern as its radiation pattern and the mode-admittance y_m as its input admittance. In the receive mode, each of the M equivalent antennas can be modeled by means of a current source with source admittance and source current i_{0m}, which in case of a spectrum $\mathbf{E}_{\text{inc}}\left(\Theta,\Phi\right)$ of homogeneous plane waves incident on the antenna becomes

$$i_{0m} = \lambda\sqrt{\frac{g_m}{\pi Z_0}}\oint \mathbf{C}_m\left(\Theta,\Phi\right)\cdot\mathbf{E}_{\text{inc}}\left(\Theta,\Phi\right)\mathrm{d}\Omega\,. \tag{7}$$

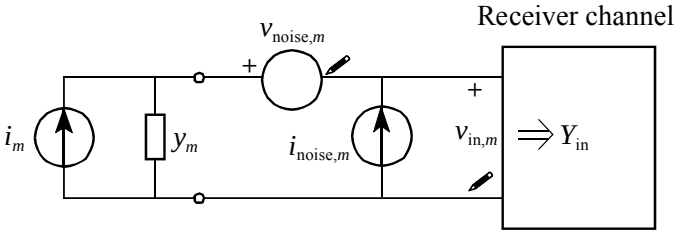

Fig. 2. Equivalent circuit for the mth eigenmode of the array antenna in receive mode. Shown is the equivalent signal current source and two noise sources representing the receiver noise.

III. DISTORTION OF RADIATION PATTERN AND POWER MISMATCH DUE TO MUTUAL COUPLING

A. Impact of different transfer functions for different eigenpatterns on DBF

For sake of simplicity, the considerations in this section and subsequent sections will be restricted to the special class of arrays as defined in Section II B. However, all conclusions derived for this special class apply to the general case as well.

The waves impinging on the array produce a set of input voltages $V_{\text{in},n}$ with n =1 to M at the input ports of the parallel

receiver channels (see Fig. 1). The digital beamformer performs a weighted linear combination (port weights W_n) of digitized output voltages $V_{\text{out},n}$. Since the output voltages are proportional to the input voltages $V_{\text{in},m}$, the beamformer response V_{beam} becomes

$$V_{\text{beam}} \sim \sum_{n=1}^{M} W_n^* V_{in,n} = \mathbf{W}^+ \mathbf{V}_{\text{in}} . \qquad (8)$$

If the array with mutually coupled elements is modeled by means of a set of equivalent current sources - each related to one eigenmode - an analog representation could be used for the set of parallel receiver channels. However, because all receiver paths are assumed to be identical and free of mutual coupling, the equivalent circuits for the receiver channels in the modal representation resemble the equivalent circuit in the port representation (see Fig. 2). The modal input voltages $v_{\text{in},m}$ are related to the input port $V_{\text{in},n}$ voltages via

$$\begin{pmatrix} v_{\text{in},1} \\ . \\ v_{\text{in},M} \end{pmatrix} = \mathbf{U}^t \cdot \begin{pmatrix} V_{\text{in},1} \\ . \\ V_{\text{in},M} \end{pmatrix}, \qquad (9)$$

with rows of the transformation matrix $\mathbf{U}$ composed of eigenvectors $\mathbf{x}_m$. Transformation of the port weights W_n into mode weights w_m according to $\mathbf{W} = \mathbf{U}\mathbf{w}$ allows the beamformer output to be expressed as $V_{\text{beam}} \sim \mathbf{w}^+ \mathbf{v}_{\text{in}}$. This relation together with (7) and consideration of the equivalent circuit in Fig. 2 (without noise sources) give

$$V_{\text{beam}} = \frac{\lambda}{\sqrt{4\pi Z_0 G_{\text{in}}}} \oint \mathbf{C}_{\text{beam}}(\Theta,\Phi) \cdot \mathbf{E}_{\text{inc}}(\Theta,\Phi) \, \mathrm{d}\Omega . \qquad (10)$$

The radiation pattern of the formed beam is given by

$$\mathbf{C}_{\text{beam}}(\Theta,\Phi) = \sum_{m=1}^{M} \Lambda_m w_m^* \mathbf{C}_m(\Theta,\Phi) . \qquad (11)$$

Eq. (11) contains the mode-specific transfer function

$$\Lambda_m = \frac{2\sqrt{g_m G_{\text{in}}}}{y_m + Y_{\text{in}}} , \qquad (12)$$

where $Y_{\text{in}} = G_{\text{in}} + jB_{\text{in}}$ denotes the input admittance of the receiver channel (see Fig. 2) . From (11), it is seen that the effective mode-weight is given by

$$\tilde{w}_m = \Lambda_m^* w_m , \qquad (13)$$

corresponding to a vector $\tilde{\mathbf{W}}$ of effective port-weights given by

$$\tilde{\mathbf{W}} = \mathbf{U} \cdot \tilde{\mathbf{w}} = \mathbf{U} \cdot \mathbf{\Lambda}^* \cdot \mathbf{w} = \mathbf{U} \cdot \mathbf{\Lambda}^* \cdot \mathbf{U}^t \cdot \mathbf{W} . \qquad (14)$$

Eqs. (11) and (12) provide a basis for examining the impact of mutual coupling on the beamforming operation. In the ideal case without coupling, all mode admittances $y_m = g_m + jb_m$ become equal to each other. Hence, the effective weights are, except for an insignificant multiplicative constant, equal to the weights used in the digital beamformer. Mutual coupling between the elements results in different transfer functions Λ_m for the different modes. If a desired radiation pattern is formed based on the uncoupled array model, the resulting radiation pattern will be distorted. However, if the transfer functions Λ_m have been determined through calibration measurements or from numerical modeling of the antenna structure, they can be compensated for in the digital domain. For this, the desired pattern is formed by adjusting the amplitude and phase of the weights in the beamformer to compensate for Λ_m.

This topic has been covered by various authors [3-7] and therefore the results and conclusions presented in this section are not new. However, it was included to clearly highlight the contrast between this type of system degeneration that can be compensated for in the digital domain, and other types (e.g. SNR reduction, discussed in section IV) that cannot be corrected for by means of digital signal processing.

B. Power mismatch considerations

Due to the orthogonality of the eigenvectors, the total power delivered to the receiver channels can be determined from the sum of the power contributions from the individual modes. The power contribution from mode m is maximized if the condition $y_m^* = Y_{\text{in}}$ (equivalent with $\Lambda_m = 1$) is met. In case of an ideal array with no mutual coupling, all mode admittances y_m are equal to each other. By utilizing two-port matching networks between antenna ports and receiver channels, the mode admittances could then be transformed to meet this condition for power matching. However, in the presence of mutual coupling, the mode admittances are not identical and simultaneous matching for all modes can principally not be achieved via two-port matching networks. If one particular mode is selected for power matching, the other modes will be mismatched. Mismatch of mode m ($\Lambda_m \neq 1$) results in a decrease in the transducer power gain for this mode relative to the case of power matching (maximum transducer gain):

$$P_{\text{out},m} / P_{\text{avail},m} = |\Lambda_m|^2 \left(P_{\text{out},m} / P_{\text{avail},m} \right)_{\max} . \qquad (15)$$

IV. SIGNAL-TO-NOISE CONSIDERATIONS

The signal-to-noise ratio (SNR) represents an important figure of merit of a receiver system. In the following consideration, it will be shown quantitatively that the degradation effects of receiver noise on the SNR are increased as a result of mutual coupling.

Noise produced in the receiver channels is superimposed on the signals produced by the waves incident at the antenna array. The noise properties of each receiver channel can be modeled by means of an equivalent noise voltage and noise current source (partially correlated to noise voltage) at the input port of the receiver channel. In the considered case, the noise signal component for receiver channel n is partially transferred to the other receiver channels $n' \neq n$ via mutual coupling, where it is amplified. This leads to a rather complicated noise analysis. However, if this noise analysis is

carried out in terms of the eigenmode representation, a very clear and simple result is obtained. It can be shown that in the equivalent circuit model for the modes (Fig. 2), noise sources can be introduced which are identical to the noise sources of the individual receiver channels.

In the noise analysis based on Fig. 2, it has to be taken into account that the effective noise temperature T_{eff} is a function of the source admittance y_m. The minimum noise temperature $T_{\text{eff,min}}$ is achieved when the source admittance equals an optimum value $Y_{\text{opt}} = G_{\text{opt}} + jB_{\text{opt}}$. The effective noise temperature for mode m becomes [8]

$$T_{\text{eff},m} = T_{\text{eff,min}} + T_0 R_{\text{eq}} \frac{\left| y_m - Y_{\text{opt}} \right|^2}{g_m}, \qquad (16)$$

with R_{eq} and T_0 denoting the equivalent noise resistance and the room temperature, respectively.

From (16), it can clearly be seen that a deviation of the mode admittance y_m from the optimum source admittance Y_{opt} results in an increased noise temperature.

If the effective weights $\tilde{w}_m$ are adjusted to form a desired radiation pattern (see eqs. (11) to (14) and the incident wave spectrum corresponding to the (desired) signal is given by $\mathbf{E}_{\text{inc}}(\Theta,\Phi)$ the SNR becomes

$$\text{SNR} \sim \frac{\sum_{m=1}^{M} \left| \tilde{w}_m \mathbf{C}_m(\Theta,\Phi) \cdot \mathbf{E}_{\text{inc}}(\Theta,\Phi) \right|^2}{T_{\text{eff,min}} \sum_{m=1}^{M} \left| \tilde{w}_m \right|^2 + T_0 R_{\text{eq}} \sum_{m=1}^{M} \left| \tilde{w}_m \right|^2 \frac{\left| y_m - Y_{\text{opt}} \right|^2}{g_m}}. \qquad (17)$$

Note that external noise contributions received by the antenna array are not taken into account in (17).

Eq. (17) provides a basis for investigating the SNR degradation due to mutual coupling. If all mode admittances were noise-matched ($y_m = Y_{\text{opt}}$ $m = 1, 2, .. M$), the second term in the nominator vanishes, resulting in the maximum SNR. However, this optimum case can only be achieved if all modes admittances are equal. For mutually coupled elements with different mode admittances, noise matching for a selected mode can only be achieved at the cost of noise-mismatch for the remaining modes. Therefore, the SNR becomes a function of the effective weights and thus a function of the formed radiation pattern. If a mode m is badly noise-matched while the desired radiation pattern requires a relatively large effective weight for the corresponding eigenpattern $\mathbf{C}_m$, the SNR is significantly reduced.

This effect cannot be compensated for by digital signal processing, and thus necessitates the use of a decoupling network, which is introduced in the following section.

V. DECOUPLING OF ANTENNA PORTS

Inter-element coupling results in deviations between the different mode admittances and this in turn precludes simultaneous power and/or noise matching by means of two-port matching networks inserted between the individual array ports and the corresponding receiver channels.

This problem can be overcome, if instead of the two-port matching networks, a 2*M*-port decoupling network (DN) is inserted with *M* input ports connected to the *M* array ports and *M* output ports connected to the receiver channel. A variety of different possible architectures for this DN are available. The principal idea is illustrated by means of Fig. 3. In Fig. 3, a DN for the example of a 3-element array and for a realization by means of lumped reactances in a generalized latter network is shown.

As seen in the example of Fig. 3, series-sections without cross-coupling (consisting of three reactances $X_{1,}$) are connected to the three array ports. This is followed by a parallel section with cross-coupling, consisting of three susceptances B_{20} and three cross-coupling elements B_2. For B_2 =0, this 6-port degenerates into three parallel 2-ports. Hence, the presence of cross-coupling elements is the key feature of a DN. In the general case with *M* elements, additional series and parallel sections may be required to achieve decoupling. For a decoupled system, the output admittances of the equivalent circuits for all modes need to have the same value. For both decoupling and matching, these admittances are required to have a specific value of Y_{in}^* (power matching) or Y_{opt} (noise matching). The values of the unknown reactances and susceptances in the DN are obtained by solving a set of non-linear equations that enforce the requirements for the real and imaginary parts of the output admittances.

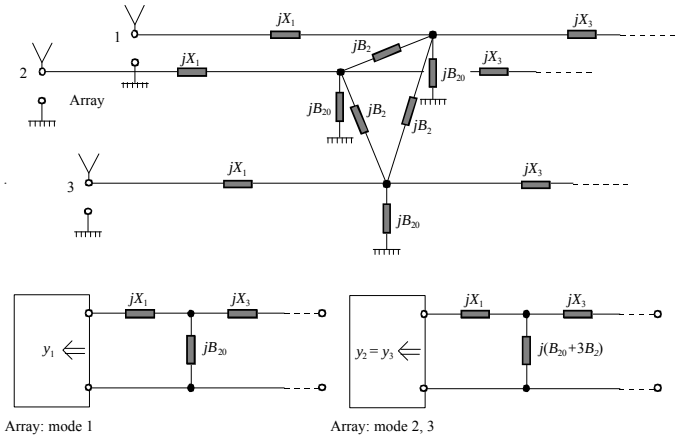

Fig. 3. Example for a decoupling network for $M = 3$ array elements. Network consists of lumped reactances in a generalized latter structure. Figure on top shows the network structure and figures below are the equivalent circuits for mode 1 and modes 2 and 3, respectively. In this case, mode admittances $y_2 = y_3$.

VI. SUPERDIRECTIVITY, BANDWIDTH AND EFFICIENCY

The pattern order N_p of an array is defined as the highest main mode number in a spherical wave approximation of the highest-order eigenpattern [9]. The conventional size d_c of an array to possess a pattern order N_p is given by $d_c \approx N_p \lambda/\pi$. If the same pattern order is produced by an array with size $d < d_c$ this array is called *superdirective*. An array with an element spacing significantly smaller than $\lambda/2$ is therefore superdirective. These highest-order eigenmodes of a superdirective array are characterized by enhanced element currents with a 180° phase change from element to element, such that even in main-beam direction, a certain amount of destructive interference occurs. A relatively large amount of reactive field energy E_r is stored in the near field of such an array, described by a high radiation quality factor $Q_{\text{rad}} = \omega E_r / P_{\text{rad}}$, which can be estimated to be

$$Q_{\text{rad}} \approx \left(d_c / d\right)^{2N_p+1}. \qquad (18)$$

Q_{rad} rapidly increases with reduced antenna size d. If dissipative losses are neglected, the maximally achievable fractional frequency bandwidth (for SWR = 2) is estimated to be [9]

$$\frac{\Delta f}{f_0} \approx \frac{1}{\sqrt{2}Q_{rad}} \frac{1.36 n_{MS}^2}{1+0.36 n_{MS}^2}, \qquad (19)$$

with n_{MS} as the number of matching sections. If the required fractional bandwidth is given, (18) and (19) can be used to estimate the maximum allowed radiation quality factor and the corresponding maximally allow size-reduction factor d_c/d. Furthermore, dissipative losses in the antenna and matching/decoupling network (up to now neglected) need to be taken into account. The radiation quality factor Q_{rad} need to be sufficiently lower than the unloaded quality factor of the structure to ensure that the reduced radiation efficiency does not negate the SNR improvements discussed in Section IV.

VII. PRACTICAL EXAMPLE

As an example, an array structure comprising of three identical monopole antennas (see Fig. 4) with a very small element spacing of $a/\lambda_0 = 0.1$ is considered [10]. The monopole length and monopole diameter were chosen as $l/\lambda_0 = 0.25$ and $d/\lambda_0 = 0.025$. Computer simulations were performed with the computer codes SuperNEC Lite [11] and Zeland IE3D [12]. Fig. 5 depicts the eigenpatterns $|\mathbf{C}_m(\pi/2, \Phi)|$, $m = 1, 2, 3$ at $f = f_0$. The maximum directivity for the three modes were computed to be $D_1 = 3.24$, $D_2 = 7.94$ and $D_3 = 7.76$. As a consequence of mutual coupling, mode admittance y_1 for the lower-order mode 1 with dipole-like radiation pattern substantially differs from the mode input admittance $y_2 = y_3$ of the degenerated higher-order modes 2 and 3. Fig. 6 shows the frequency dependence of the modal admittances as a function of the normalized frequency $F = f / f_0 = 4lf/c$. The low-order and higher-order modes resonate at different frequencies, but the most notable difference is in the radiation quality factor Q_{rad}, where the higher-order modes display a significantly higher value.

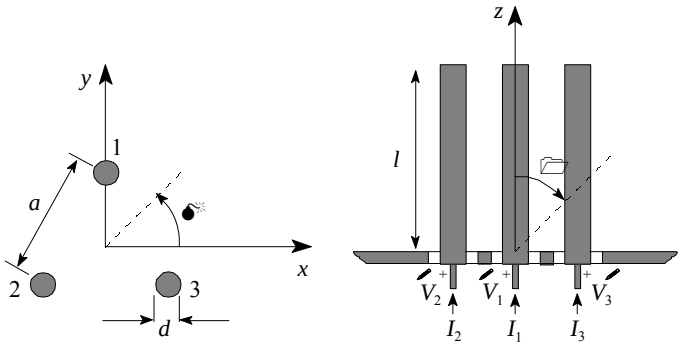

Fig. 4. Considered 3-element array with monopole elements (height l, diameter d) and element spacing a. Here: $a = 0.1\ \lambda_0$ and $l = 0.25\ \lambda_0$.

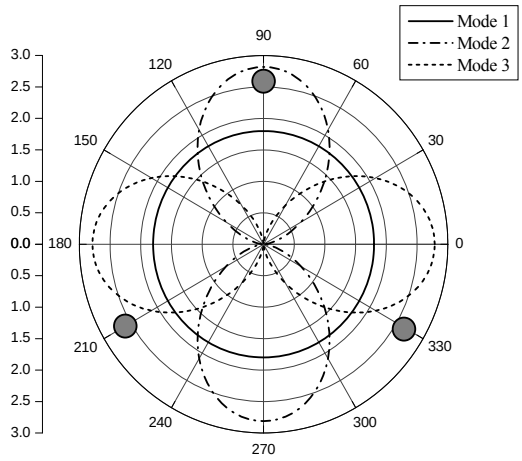

Fig. 5. Normalized radiation patterns of the three eigenmodes $|\mathbf{C}_m(\pi/2, \Phi)|$, $m = 1, 2, 3$.

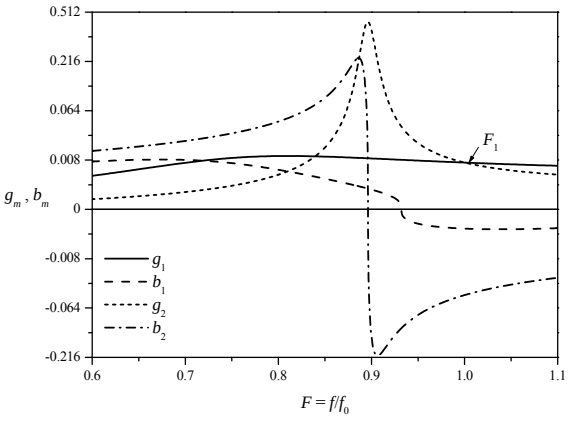

Fig. 6. Computer simulation results for the frequency response of real and imaginary part of the mode admittance y_1 for the low-order and $y_2 = y_3$ of the higher-order modes. F_1 indicates values of the normalized frequency where the conductance $g_1 = g_2$.

The point indicated as F_1 in Fig. 6 corresponds with the normalized frequency where $g_1 = g_2$, or equivalently, $Y_{12} = jB_{12}$. At this operational point, the coupling between the array elements becomes purely reactive. This has the advantage of simplifying the decoupling network architecture. In general, a symmetrical 3-element array would only require elements X_1 and B_2 in the DN of Fig. 3. However, for the operational point F_1 where $Y_{12} = jB_{12} = j0.0151\ \Omega^{-1}$, the DN is further simplified in that X_1 becomes redundant (i.e. $X_1 \approx 0$), while $B_2 = B_{12} = 0.0151\ \Omega^{-1}$. The decoupling network thus reduces to capacitive cross coupling between adjacent antenna ports with a capacitance of $C = 0.0151/\omega_0$ F. With this simple decoupling network, ports 1 to 3 become decoupled at F_1. This results in a decoupled port impedance of $1/\tilde{Y}_1 = 1/\tilde{Y}_2 = 140.3 - j2.27\ \Omega$, which may easily be transformed into the desired load impedance, e.g. $Z_{\text{in}} = 50\,\Omega$. The frequency bandwidth of decoupling and matching for this case is indicated in Fig. 7, which shows the frequency response of $|\tilde{S}_{11}|^2$ (fraction of power reflected) and $2|\tilde{S}_{21}|^2$ (fraction of power coupled to the loads at the other two ports). Note that the loss due to reflection and cross coupling is theoretically zero at the center frequency. If the frequency bandwidth is defined via the requirement that 89 % of the power incident to the array is to be radiated (equivalent with the VSWR<2 bandwidth for single antennas), a fractional bandwidth of 2.6% is observed.

If a wave is fed into port 1 of the decoupled array while the other two ports are terminated in matched loads, a linear combination of modes 1 and 2 is excited, resulting in a radiation pattern

$$\mathbf{C}_{\text{Port1}}(\Theta,\Phi) = \left(\mathbf{C}_1(\Theta,\Phi) + \sqrt{2}\mathbf{C}_2(\Theta,\Phi)\right)/\sqrt{3}\,, \qquad (20)$$

with a maximum directivity of $|\mathbf{C}_{\text{Port1}}|^2_{\max} = 10.41$. Fig. 8 depicts the azimuth pattern for $\Theta = \pi/2$. If port 2 or 3 is excited, the radiation pattern is rotated about the z-axis by ± 120 degrees.

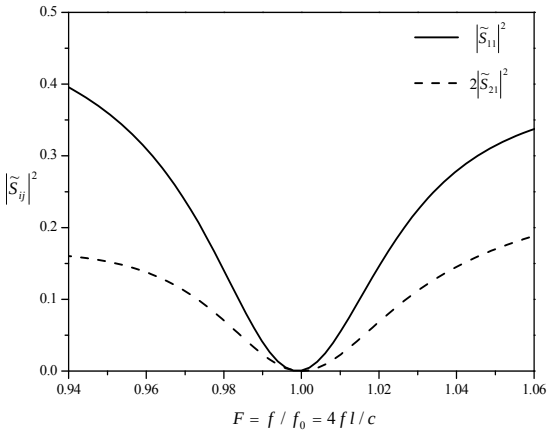

Fig. 7. Computer simulation results for the effectiveness of decoupling and matching. Shown is the fraction of power reflected and power coupled to other ports as a function of frequency when feeding one port of an array with $a/\lambda_0 = 0.1$, $d/\lambda_0 = 0.025$ and monopole length of $l/\lambda_0 \approx 0.25$.

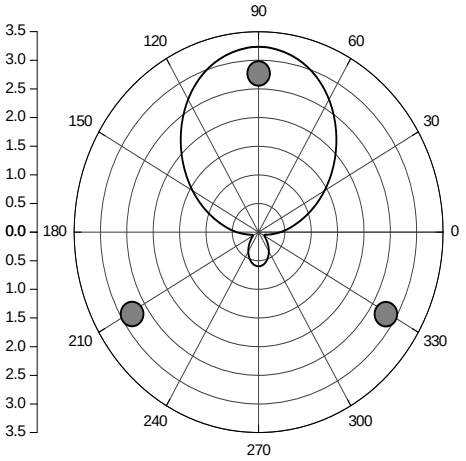

Fig. 8. Radiation pattern $|\mathbf{C}_{\text{Port 1}}(\pi/2,\Phi)|$ at frequency f_0 obtained by feeding port 1 of the 3-element array with attached decoupling network.

These radiation patterns are characterized by the fact that even in direction where the maximum directivity occurs, a partially destructive interference between the field contributions of the monopole currents occurs. This is therefore a superdirective array [2,9,13]. The monopole elements together with the RF-DN form a resonator that provides the resonant current enhancement needed for superdirective radiation properties.

REFERENCES

[1] J. Litva and T.K.Y. Lo, *Digital Beamforming in Wireless Communications,* Norwood: Artech House,1996.

[2] R.C. Hansen, *Phased Array Antennas*, New York: Wiley, 1998.

[3] I.J. Gupta and A.A. Ksienski,"Effect of mutual coupling on the performance of adaptive arrays", *IEEE Trans. Antennas Propagation*, vol. 31, pp. 785-791, 1983.

[4] P. Darwood, P.N. Fletcher, and G.S. Hilton, "Mutual coupling compensation in small planar array antennas", *IEE Proc. Microwaves, Antennas Propagation*, vol. 145, pp. 1-6, 1998.

[5] H. Steyskal and J.S. Herd,"Mutual coupling compensation in small array antennas," *IEEE Trans. Antennas Propagation*, vol. 38, pp.1971-1975, 1990.

[6] R.S. Adve and T.K. Sarkar, "Compensation for the effects of mutual coupling on the direct data domain adaptive algorithms", *IEEE Trans. Antennas Propagation*, vol. 48, pp.86-94, 2000.

[7] B. Friedlander and A.J. Weiss, "Direction finding in the presence of mutual coupling", *IEEE Trans. Antennas Propagation*, vol. 39, pp.273-284, 1991.

[8] H.A. Haus,"Representation of noise in linear two-ports", *Proc. IRE*, pp. 69-74, 1960.

[9] H.J. Chaloupka, "HTS antennas",in H. Weinstock and M. Nisenoff (eds.), *Microwave Superconductivity*, Dordrecht: Kluwer 2001

[10] H.J. Chaloupka, X. Wang and J.C. Coetzee," Superdirective 3-element array for adaptive beamforming", submitted for publication.

[11] SuperNEC Lite, Version 2.0, Poynting Software Pty. Ltd.

[12] IE3D, Version 9.16, Zeland Software Inc.

[13] R.C. Hansen,"Fundamental limitations in antennas", *Proc. IEEE*, vol. 69, pp. 170-182, 1981.